Proceedings of the XXXI International School of Semiconducting Compounds, Jaszowiec 2002

Femtosecond Dynamics of Neutral and Charged Exciton Absorption in $Cd_{1-x}Mn_xTe$ Quantum Well

P. Płochocka[a], P. Kossacki[a,*], W. Maślana[a], C. Radzewicz[a], J.A. Gaj[a], J. Cibert[b] and S. Tatarenko[b]

[a]Institute of Experimental Physics, Warsaw University
Hoża 69, 00-681 Warsaw, Poland
[b]Laboratoire de Spectrométrie Physique, CNRS
et Université Joseph Fourier – Grenoble
B.P. 87, 38402 Saint Martin d'Heres Cedex, France

We present a study of time-dependent transmission spectra of a modulation-doped $Cd_{1-x}Mn_xTe/Cd_{1-y-z}Zn_yMg_zTe$ quantum well with variable hole gas concentration. We study the influence of pump pulses on excitonic absorption in subpicosecond time scale. A spectrally broad probe pulse of duration of 40 femtoseconds was used to record the absorption spectra at controlled delay. Studies of temporal evolution of exciton energies revealed coherence decay of linearly polarized excitons and thermalization of non-equilibrium exciton states. We found that a characteristic timescale for thermalization of non-equilibrium populations of photocreated excitons is between 0.8 and 3.6 ps. The timescale of this process depends on the hole concentration in quantum well: for higher hole concentration the decay is faster. Long-lived photo-induced magnetization accompanied by heating of the magnetic system was also observed.

PACS numbers: 78.40.Fy, 78.47.+p, 78.67.De

1. Introduction

The spectroscopy of quantum wells containing moderate concentration of carriers has been studied extensively during last years. It is known that the optical spectra near energy gap are dominated by two sharp lines related to neutral and

*corresponding author; e-mail: kossacki@fuw.edu.pl

charged excitons [1–7]. These transitions are observed in different experimental configurations such as absorption, photoluminescence, Faraday rotation, four wave mixing (FWM), etc. So far extensive studies of their properties were carried out in both continuous wave (CW) [1–3, 7] and time-resolved experiments [8, 9, 6, 10].

The time-resolved studies were mostly focused on the timescale from several to hundred of picoseconds. Such range is a proper scale for charged exciton formation from neutral excitons and carriers [11] as well as the radiative recombination [9, 10] or spin flip processes. In the present work we focused on subpicosecond timescale. In order to obtain such temporal resolution we performed pump-probe experiment with the laser pulse of duration of 40 fs.

2. Sample and experiment

The present study was carried out on a modulation doped structure consisting of a single 80 Å quantum well (QW) of $Cd_{1-x}Mn_xTe$ ($x \approx 0.0018$) embedded between $Cd_{0.66}Zn_{0.27}Mg_{0.07}Te$ barriers grown pseudomorphically on a (100) $Cd_{0.88}Zn_{0.12}Te$ substrate. Modulation p-doping was assured by a nitrogen-doped layer placed at 200 Å from the QW. The hole gas concentration in the QW was controlled by an additional illumination provided by a tungsten halogen lamp with a blue filter. The mechanism of the hole gas concentration control in the QW is described in detail in [3]. The experiment was performed in a typical pump-probe configuration (see Fig. 1). Pump and probe femtosecond pulses separated by a con-

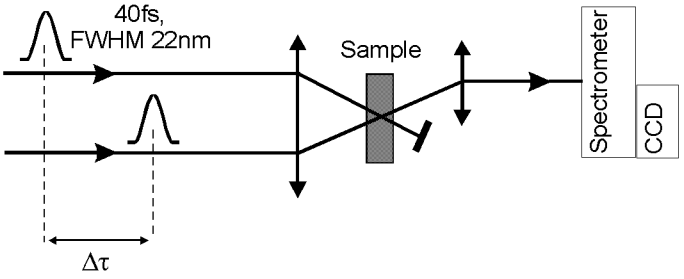

Fig. 1. Pump-probe experiment. Two femtosecond pulses are focused on the sample. The strong one (pump pulse) is blocked after the sample and the spectrum of the weaker one (probe pulse) is recorded as a function of delay between both pulses, which is controlled independently. Duration of the pulse is about 40 fs; the spectrum of width 22 nm (FWHM) is centered at 760 nm.

trolled delay were focused on the sample to a common spot of a diameter smaller than 100 μm. The angle between the two beams was about 5°. The pulses were generated by a Ti^{3+}:Al_2O_3 laser at a repetition rate of 100 MHz. They had duration of 40 fs, spectral width 22 nm, and were centered at 765 nm. The power of both pulses was controlled independently, the pump-to-probe ratio being at least

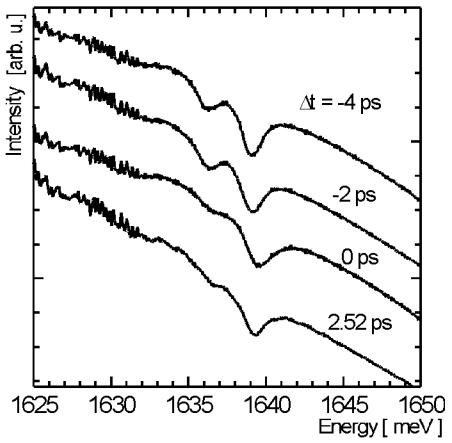

Fig. 2. Transmission spectra for four different delays between pump and probe pulses. Two upper spectra are for negative delays — the probe pulse precedes the pump pulse. Two absorption lines related with neutral and charged exciton are clearly visible. At zero delay both pulses reach the sample at the same time.

20:1. The average power of the pump beam was typically 16 mW which is equivalent to creation of about 6×10^{10} cm^{-2} excitons in each pulse. The spectrum of the probe pulse transmitted through the sample was recorded as a function of delay between pump and probe pulses. Time resolution was 40 fs. The sample was mounted strain-free in a superconducting magnet and immersed in superfluid helium. The temperature was 1.8 K. The measurements in magnetic field were done in the Faraday configuration. Typical spectra for four different delays are shown in Fig. 2.

In some experiments the pump beam was polarized circularly. The circular polarization of the pump pulse selects different transitions between spin subbands: polarization σ^+ creates electrons in conduction band with spin value $-1/2$ and holes in valence band with angular momentum value $+3/2$. For opposite circular light polarization also the values of the hole and electron angular momentum are opposite. The probe beam was polarized linearly and detected after the sample at both circular polarizations. Linear polarization of the pump pulse was also used in some other experiments.

3. Temperature of the manganese system

The intense pump pulses warm up the sample. Due to this fact we found the temperature of the manganese ions varying as a function of power of the pump pulse. To determine the temperature of the Mn spins, measurements of the Zeeman effect were done with a CW light source. Standard transmission of light obtained from the halogen lamp was measured under illumination with a strong pump beam. The Zeeman effect reflects averaged magnetization of CdMnTe material in QW

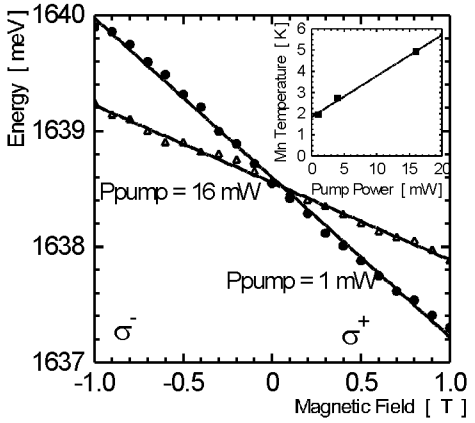

Fig. 3. Zeeman splitting for different powers of the pump pulse: 16 mW (rectangles) and 1 mW (circles). The inset shows the dependence of the temperature of the Mn ions on power of the pump pulse.

[12–14]. In Fig. 3 the energy of the neutral exciton versus magnetic field (Zeeman effect) is presented. The magnetic field was changed between +1 T and –1 T. The presented data were obtained for different powers of the pump beam. We found the temperature of the Mn ions about 4.9 K at 16 mW pump beam power (rectangles in Fig. 3) and $\approx$ 2 K at 1 mW (circles). The Mn spin temperature is plotted in the inset in Fig. 3 versus pump beam power.

4. Photoinduced magnetization

It is known that circularly polarized light can induce magnetization in diluted magnetic semiconductors [15]. Due to this fact for a circularly polarized pump beam a Zeeman splitting should be observed for both excitonic absorption

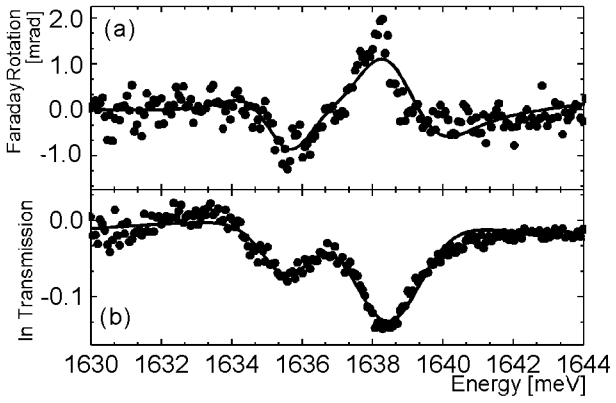

Fig. 4. Faraday rotation versus photon energy at delay of –4 ps (a). Transmission of the sample (b). The continuous lines were obtained from fitting.

lines between the two circular polarizations of the probe beam. To find the value of this photoinduced magnetization the Faraday effect was measured [7]. This measurement was done for delay –4 ps (the probe pulse was reaching the sample 4 ps before the pump pulse and about 10 ns after the previous one). At that moment all carriers created by the previous pump pulse have already recombined [9] and there is no direct modification of absorption by the photocarriers.

Figure 4 shows the Faraday rotation as a function of photon energy (upper panel) and the average σ^+/σ^- transmission spectrum (lower panel). The rotation is observed due to the Mn magnetization created by the previous pump pulse. From Faraday rotation we found the splitting and difference between oscillator strength of neutral and charged exciton between the two circular polarizations of the probe beam. We use the X-splitting to determine the photoinduced magnetization, obtaining 0.56% in units of saturation magnetization at 16 mW pump power.

5. Evolution of X energy — blue shift

The behavior of both excitonic absorption lines was investigated for linear polarization of the pump beam and the same polarization of the probe beam. At zero delay a significant blue shift of both exciton lines was observed, gradually disappearing thereafter. Gaussian fits of both lines allowed us to determine temporal evolution of their energy positions and intensities. Figure 5 represents neutral exciton energy versus delay of the probe pulse relative to the pump pulse, measured

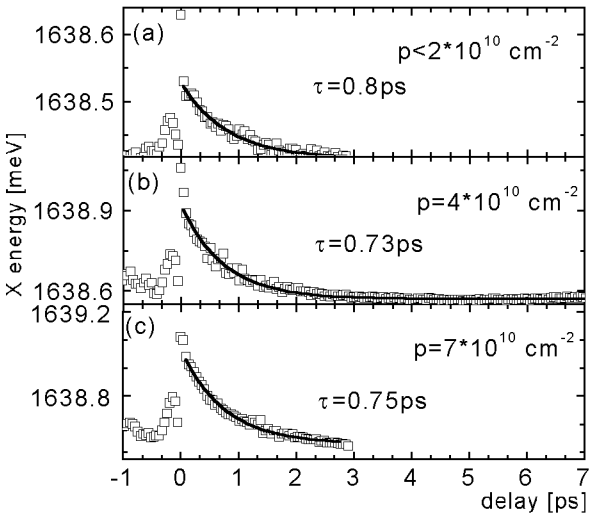

Fig. 5. Energy shift versus delay for neutral exciton. The open squares are the experimental data. Solid lines represent fitted exponential functions. p denotes hole concentration: (a) $p < 2 \times 10^{10}$ cm^{-2}, (b) $p = 4 \times 10^{10}$ cm^{-2}, (c) $p = 7 \times 10^{10}$ cm^{-2}. τ is the characteristic decay time found from fitting exponential functions to the data.

for different hole concentrations ((a) $p < 2 \times 10^{10}$ cm^{-2}, (b) $p = 4 \times 10^{10}$ cm^{-2}, (c) $p = 7 \times 10^{10}$ cm^{-2}).

The X energy shift decays exponentially with characteristic time smaller than 1 ps independently of the hole concentration. The linearly polarized pump pulse excites a coherent combination of both excitonic spin states. Decay of coherence of these states contributes to the observed decay of the blue shift.

6. Exciton thermalization

A similar experiment was performed for circular polarization of the pump pulse. The initially linearly polarized probe pulse was detected in both circular polarizations. The difference between two circular polarizations of the probe pulse in neutral exciton line position — the X splitting — for different hole concentrations is presented in Fig. 6 versus delay.

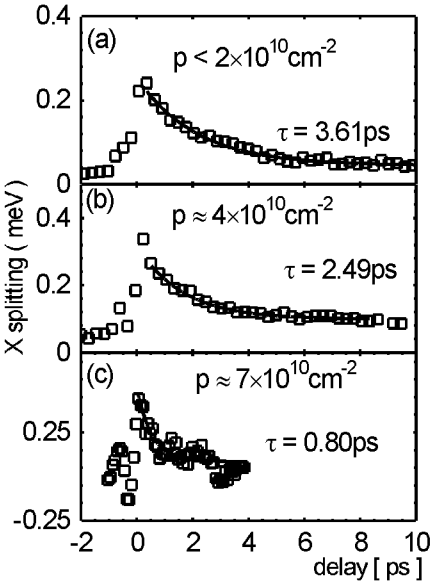

Fig. 6. Exciton splitting versus delay between pump and probe pulses for different hole concentrations: (a) $p < 2 \times 10^{10}$ cm^{-2}, (b) $p = 4 \times 10^{10}$ cm^{-2}, (c) $p = 7 \times 10^{10}$ cm^{-2}. The points are the experimental data. Solid lines represent fitted exponential functions. τ is characteristic decay time obtained from fits.

For negative delays the value of X splitting is constant and related to the photoinduced magnetization, previously discussed. For delay equal to zero the splitting grows up rapidly, and then decays exponentially with time constant decreasing with hole concentration from 3.6 ps to about 0.8 ps. The origin of the X splitting can be explained in the following way: the pump pulse creates a non-equilibrium population of excitons. When the polarizations of pump and probe

pulses are the same, phase space blocking makes the binding energy of excitons smaller. For opposite polarizations of pump and probe pulses only (polarization independent) screening effects remain. The decay of the X splitting is a relaxation of non-equilibrium population of excitons created in the QW by the pump pulse. The observed strong influence of the carrier concentration suggests important role of the Coulomb interactions with carriers present in the QW.

7. Conclusions

We observed a strong influence of the pump pulse on excitonic absorption in the quantum well on subpicosecond timescale. Long-lived photoinduced magnetization accompanied by heating of the magnetic system was also observed. Studies of temporal evolution of exciton energies revealed coherence decay of linearly polarized excitons and thermalization of non-equilibrium exciton states.

Acknowledgments

This work was partially supported by the State Committee for Scientific Research, Poland (grants 2P03B09418 and 5P03P02320) and by Polish-French collaboration program Polonium.

References

[1] K. Kheng, R.T. Cox, Y. Merle d'Aubigné, F. Bassani, K. Samindayar, S. Tatarenko, *Phys. Rev. Lett.* **71,** 1752 (1993).

[2] T. Wojtowicz, M. Kutrowski, G. Karczewski, J. Kossut, F.J. Teran, M. Potemski, *Phys. Rev. B* **59,** R10437 (1999).

[3] P. Kossacki, J. Cibert, D. Ferrand, Y. Merle d'Aubigné, A. Arnoult, A. Wasiela, S. Tatarenko, J.A. Gaj, *Phys. Rev. B* **60,** 16018 (1999).

[4] G. Finkelstein, H. Shtrikman, I. Bar-Joseph, *Phys. Rev. Lett.* **74,** 976 (1995).

[5] G.V. Astakhov, D.R. Yakovlev, V.P. Kochereshko, W. Ossau, J. Nürnberger, W. Faschinger, G. Landwehr, *Phys. Rev. B* **60,** 8485 (1999).

[6] D. Brinkmann, J. Kudrna, P. Gillot, B. Hönerlage, A. Arnoult, J. Cibert, S. Tatarenko, *Phys. Rev. B* **60,** 4474 (1999).

[7] W. Maślana, W. Mac, J.A. Gaj, P. Kossacki, A. Golnik, J. Cibert, S. Tatarenko, T. Wojtowicz, G. Karczewski, J. Kossut, *Phys. Rev. B* **63,** 165318 (2001).

[8] G. Finkelstein, V. Umansky, I. Bar-Joseph, V. Ciulin, S. Haacke, J.D. Ganiére, B. Deveaud, *Phys. Rev. B* **58,** 12637 (1998).

[9] E. Vanelle, M. Paillard, X. Marie, T. Amand, P. Gilliot, D. Brinkmann, R. Lévy, J. Cibert, S. Tatarenko, *Phys. Rev. B* **62,** 2696 (2000).

[10] V. Ciulin, P. Kossacki, S. Haacke, J.D. Ganiére, B. Deveaud, A. Esser, M. Kutrowski, T. Wojtowicz, *Phys. Rev. B* **62,** R16310 (2000).

[11] P. Kossacki, A. Kudelski, J.A. Gaj, J. Cibert, S. Tatarenko, D. Ferrand, A. Wasiela, B. Deveaud, T. Dietl, *Physica E* **12,** 344 (2002).

[12] J.A. Gaj, W. Grieshaber, C. Bodin-Deshayes, J. Cibert, G. Feuillet, Y. Merle d'Aubigné, A. Wasiela, *Phys. Rev. B* **50,** 5512 (1994).

[13] J. Spalek, A. Lewicki, Z. Tarnawski, J.K. Furdyna, R.R. Galazka, Z. Obuszko, *Phys. Rev. B* **33,** 3407 (1986).

[14] A.V. Scherbakov, D.R. Yakovlev, A.V. Akimov, I.A. Merkulov, B. König, W. Ossau, L.W. Molenkamp, T. Wojtowicz, G. Karczewski, G. Cywinski, J. Kossut, *Phys. Rev. B* **64,** 155205 (2001).

[15] H. Krenn, W. Zawadzki, G. Bauer, *Phys. Rev. Lett.* **55,** 1510 (1985).